

## EXPERIMENTAL CHARACTERIZATION OF WIRELESS MIMO CHANNEL AT 5.8 GHz IN UNDERGROUND GOLD MINE

Bilel Mnasri<sup>1</sup>, Mourad Nedil<sup>1, \*</sup>, Nahi Kandil<sup>1</sup>, Larbi Talbi<sup>2</sup>, and Ismail Ben Mabrouk<sup>2</sup>

<sup>1</sup>Underground Communications Research Laboratory, UQAT, Val-d'Or, Canada

<sup>2</sup>Department of Computer Science and Engineering, UQO, Gatineau, Canada

**Abstract**—This paper presents analysis results relative to an underground MIMO channel. Measurement campaigns were conducted in a former gold mine at a center frequency of 5.8 GHz under Line-Of-Sight (LOS) scenario. Extracted data have been processed to obtain the relevant statistical parameters of the channel. The resulting propagation behavior differs from frequently encountered in more typical indoor environments, such as offices and corridors. Indeed, the path loss exponent is less than 2 in MIMO configuration due to the large number of scatters that increase the received power when compared to the free-space case. Moreover, there has been a significant increase in spectral efficiency, when using MIMO technique. Hence, according to calculated statistical parameters, wireless link performance is improved through the use of the MIMO scheme. All in all, multi antenna systems present an ideal alternative for future underground communication systems.

### 1. INTRODUCTION

In wireless communications, the channel characterization has enjoyed renewed interest. In fact, the experimental channel sounding and the extraction of the overall behavior is a key feature and a relevant task in order to have an accurate understanding of the propagation phenomena. From a practical point of view, the channel characterization gives engineers, as well as researchers, guidelines to

---

*Received 27 November 2012, Accepted 11 January 2013, Scheduled 19 January 2013*

\* Corresponding author: Mourad Nedil (mourad.nedil@uqat.ca).

conceive the most efficient communication systems. Indeed, these guidelines are suggested from the channel sounding results.

For many decades, wire-based communication systems have been the only method of getting connected to manufacturers' staffs working in underground environments like tunnels or mines. Such systems were not able to resist in case of disasters. In addition, it was difficult and very expensive for these systems to be extended in some underground areas. Therefore, wireless technology has been the chosen candidate to be used as the next generation in underground areas. In fact, unlike wire-based systems, wireless technology is more resistant in natural catastrophes. Furthermore, it is easier to extend wireless communication systems in those unclassical environments.

Underground environments, and particularly mines, are rich of scatters, which create the space diversity through uncorrelated paths between the transmitter and the receiver as it was proved by the work of Ben Mabrouk et al. [1]. To take benefit from multipaths present in such environments, MIMO technique has been chosen. In fact, MIMO channel capacity increases with diversity [2]. Hence, multi antenna technique is a key feature in communication systems implemented in mines and tunnels. The additional capacity gained through higher rank channel matrices can be used to improve the transmission rate or the reliability of the wireless link [3, 4].

Many studies have been dealing with radio wave propagation behavior in indoor environments. In fact, in [5,6] MIMO channels were investigated within closed buildings at 5.2 GHz. The goal was to define the possibilities of implementing wireless LAN standards in combination with MIMO in closed areas. Ben Mabrouk et al. have demonstrated in many studies the potential of multiantenna systems within underground mine galleries at 2.4 GHz and in the UWB frequency range [1, 11, 13]. Wireless underground SISO systems were also characterized at 5.8 GHz by Boutin et al. in [7]. But for the best of our knowledge, no such studies have been conducted for MIMO channels at 5.8 GHz in mine galleries.

The objective of this paper is to characterize experimentally an underground propagation channel using  $2 \times 2$  MIMO antenna system at 5.8 GHz. Performance comparison with SISO systems is also presented. The main propagation parameters, such as, path loss, correlation, channel capacity and Ricean  $K$ -factor were extracted from experimental results. This work contributes to communication applications of MIMO technology, aiming at operational enhancements and safety for the mining industry.

This work is organized as follows. Section 2 gives a brief description of the underground mining environment as well as

the experimental setup and the measurement campaign procedure. Experimental results are studied and discussed in Section 3. Finally, Section 4 concludes the paper.

## 2. EXPERIMENTAL PROTOCOL

### 2.1. Description of the Mining Environment

Experimental measurements were conducted in a real underground gallery of a former gold mine. This mine-laboratory is actually operated by the Canadian Center for Minerals and Energy Technology (CANMET) in northern Canada. The gallery is located at a 40 m depth, and it stretches over a length of 70 m with a width of 2.5 to 3 m and is approximately 3 m in height. The floor is flatter than the ceiling and the walls with very rough surfaces, and contains some water puddles. There is still high humidity as well as some pools of water covering the ground. The temperature is varying in between 6°C and 17°C along the year. A digital photography of the underground mine gallery is shown in Fig. 1.

### 2.2. Channel Sounder Setup

The results presented in this study are based on radio channel measurements using an Agilent E8363B-Vector Network Analyzer (VNA). The sounding system consists mainly of the sets of Vivaldi antennas that have been introduced in [1], one power amplifier at the transmitter and one Low Noise Amplifier at the receiver with 30 dB of gain each, as well as two RF switches as shown in Fig. 3. The calibration is performed at 1 m separation between the transmitting



**Figure 1.** Digital photograph of the underground mine gallery.

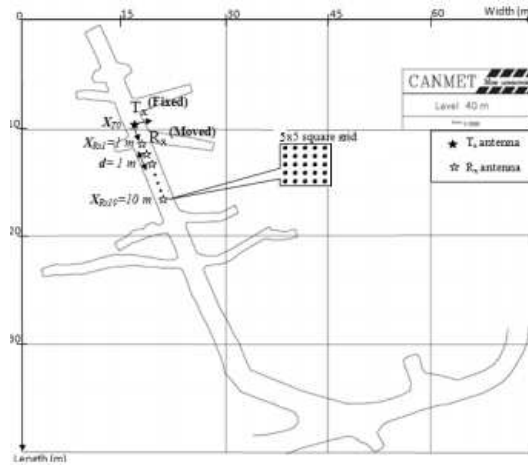


Figure 2. Map of the underground gallery.

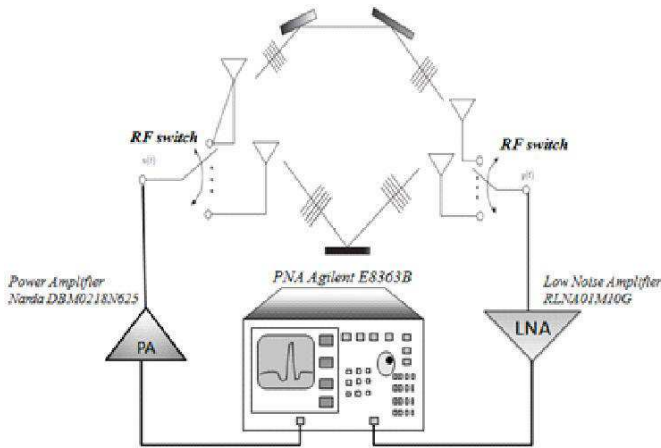


Figure 3. Measurement setup.

and the receiving antennas. This 1 m Tx-Rx separation  $d_o$  is picked to be the reference distance for the path loss modeling. This process of calibration is necessary to remove additional antenna gains and losses introduced through cables from the measured frequency response  $S_{21}$ . Hence, the data collected through measurement campaigns will describe the channel behavior without external or parasitic effects.

The frequency sampling interval was chosen to be  $\Delta_f = 1\text{ MHz}$  and the measurements were performed in the frequency range between 5.7 and 5.9 GHz (BW = 200 MHz).

During the channel sounding, the transmitter was remained fixed,

while the receiver was changing its position with 1 meter step. At each position, the channel measurements were averaged in accordance to the set of data collected on  $5 \times 5$  square grid with a distance resolution  $\Delta_d = 5$  cm as shown in Fig. 2. Measurements were also conducted with minimal human movement and activity so that the channel can be considered quasi-static.

In our measurement campaign, the inter-element distance for the transmitter and the receiver antenna sets was chosen to be one half wavelength relatively to the operating center frequency  $f_c = 5.8$  GHz. In fact, in both the transmitter and the receiver side, antennas were  $\lambda/2 = 2.6$  cm apart. This distance is highly recommended in order to ensure a minimum achievable correlation between receive signals in the MIMO system [8].

### 3. EXPERIMENTAL RESULTS

#### 3.1. Power Delay Profile

The channel impulse response  $h(t)$  is obtained using the Inverse Fourier Transform (IFT) of the channel frequency response given by the scattering parameter  $S_{21}$  [11]. The Power Delay Profile is usually used to provide information about the noise floor and the multipath strength in the environment of measurements. The first arrival delay  $\tau_{direct}$  given in the signal PDF corresponds to the first received path which is usually the Line-Of-Sight (LOS). The first path is generally set as a reference for the other measured delays as depicted in Fig. 4.

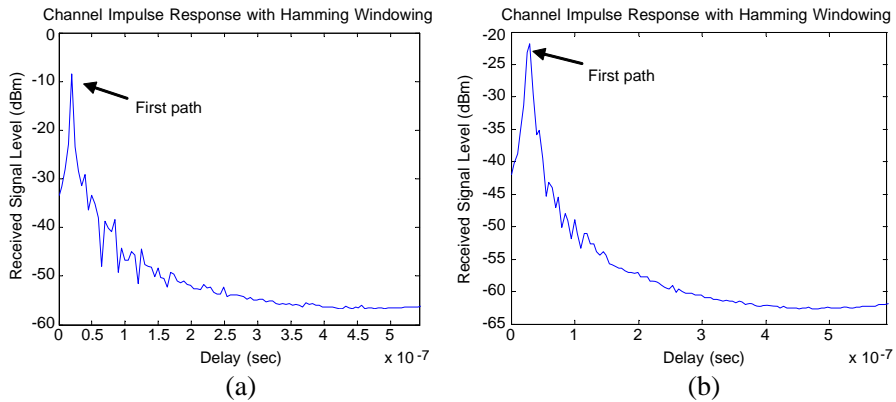


**Figure 4.** Received power level for (a)  $d_{TX-RX} = 4$  m: MIMO-LOS, and (b)  $d_{TX-RX} = 10$  m: MIMO-LOS.

As shown in both Fig. 4(a) and Fig. 4(b) respectively, the first path in the channel impulse response is equivalent to the direct signal in the LOS configuration. Indeed, in Fig. 4(a) the first signal arriving at the receiver was captured at a delay equals to 13 ns. This delay corresponds to the TX-RX distance of 4 meters. Similarly for Fig. 4(b) the first path delay of approximately 33 ns which corresponds to the 10 meters distance between the transmitter and the receiver.

### 3.2. Rician $K$ -factor

In wireless communications, the relative strength of the direct and scattered components of the received signal, as expressed by the Rician  $K$  factor, provides an indication of link quality [9]. Accordingly, efficient and accurate estimation of this parameter is of considerable interest. Indeed, it serves in general channel characterization, adaptive modulation as well as link budget calculations. In addition, it has been proved through a variety of studies that MIMO systems performances are highly correlated to the Rician factor range. In fact, it is demonstrated in [10] that at a fixed Signal to Noise Ratio (SNR), higher  $K$ -factor refers to greater spatial correlation and hence a reduction in terms of MIMO capacity.

The Rician factor describes the relative strength of the direct path signal power to that of scattered components. As it was presented in [11, 12], it is computed for each of the  $2 \times 2$  MIMO sub-channels ( $h_{mn}$ ;  $m, n = 1 : 2$ ) and then an average is made to obtain its value for the MIMO system. The Rician factor is expressed for each subchannel

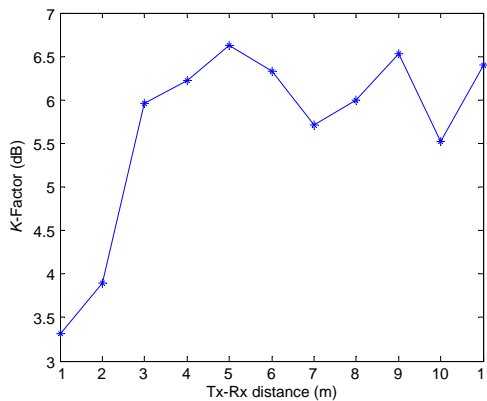


**Figure 5.** The Rician  $K$ -factor versus Tx-Rx separation distance.

**Table 1.** Statistics of the  $K$ -factor inside the mine gallery (minimum, maximum, average and standard deviation measured values).

	Min	Max	Mean	std
$K$ -factor	3.31	6.62	5.68	1.08

$h_{mn}$  as follows.

$$K \text{ (dB)} = \left( \frac{\epsilon (|h_{mn}|)^2}{2\text{var}(|h_{mn}|)} \right) \quad (1)$$

where  $\epsilon$  denotes the mathematical expectation (average) and  $\text{var}$  refers to the variance of subchannel vector  $h_{mn}$ . As shown in Fig. 5. The Rician factor increases with distance. In fact, as long as the separation between the transmitter and the receiver goes up, the scattered components are going to encounter more and more reflections against the walls, the ceiling as well as the floor. Hence, the ratio of the direct path energy to the diffused multipath power will increase. Table 1 gives statistics relative to this parameter inside the gold mine gallery.

### 3.3. Path loss

In wireless communications, the path loss of radio waves influences the received power and the link budget of the whole system. In addition, the path loss provides relevant information needed when performing the design of any wireless communication system. In this paper, the path loss, at a given distance  $d$  between the transmitter and the receiver, is given by applying the following formula [13].

$$Pl(d)_{\text{dB}} = \frac{1}{M} \frac{1}{N} \sum_{i=1}^M \sum_{j=1}^N |f(i, j, d)|^2 \quad (2)$$

where  $|f(i, j, d)|$  is the complex frequency response of the channel,  $M$  the number of measured frequency points, and  $N$  the size of the grid used to obtain an average of the local path loss. In our study,  $M$  and  $N$  are chosen to be 201 and 25 respectively.

Moreover, we assume that path loss follows the Log distance model with lognormal shadowing. Hence, in the undertaken mine gallery, the path loss at a distance  $d$  is expressed as [14]:

$$Pl(d)_{\text{dB}} = \overline{Pl(d_0)_{\text{dB}}} + 10\alpha \log \left( \frac{d}{d_0} \right) + X_\sigma \quad (3)$$

where  $\overline{Pl(d_0)_{\text{dB}}}$  is the average path loss at the reference distance  $d_0 = 1$  m,  $10\alpha \log(\frac{d}{d_0})$  is the mean path loss referenced to  $d_0$ ,  $\alpha$  is the

path loss exponent. And  $X_\sigma$  is a zero mean Gaussian random variable representing the lognormal shadowing. Furthermore, it is important to notice that the mean path loss at the reference distance  $d_0$  as well as the path loss exponent  $\alpha$ , were estimated using least square regression analysis.

The average received power as depicted in Fig. 6 is computed, at each distance, by averaging levels of the four signals that exist between the two transmitting antennas (Tx1, Tx2) and the two receiving antennas (Rx1, Rx2). Moreover, the statistical parameters of the pathloss in the undertaken mine gallery were calculated and results are given in Table 2. Indeed, in terms of large scale effect, the pathloss exponent is found to be equal to  $\alpha = 2.1$  which is close that reported by Boutin et al. in [7].

### 3.4. MIMO Channel Capacity

The channel capacity is defined as the highest transfer rate of information, which is allowed to be transmitted with a low arbitrary error probability [15]. For MIMO systems, the system capacity depends highly on the statistical properties of the channel matrix. In

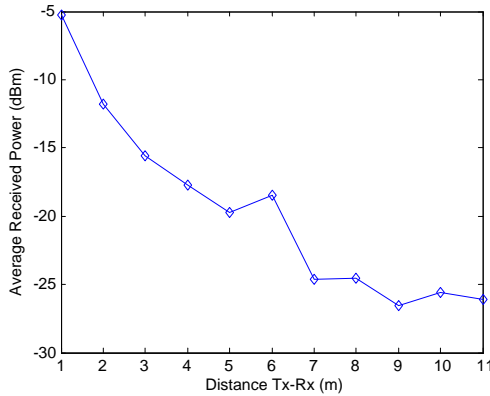


**Figure 6.** Average received power versus distance.

**Table 2.** Mean received power at the reference distance, path loss exponent and standard deviation of the random variable  $X$ .

	Average received power at distance $d_0$ (dBm)	$\alpha$	$\sigma_X$ (dB)
Statistics	-5.28	2.1	3.12

fact, under a flat fading channel, and for a fixed transmitted power configured at 10 dBm and a noise floor of  $-110$  dBm, with no channel state information (CSI) at the receiver, the  $M \times N$  MIMO channel capacity can be expressed by (4), assuming the transmitted power to be uniformly distributed among the  $N$  transmitting antennas [16].

$$C = \log_2 \left( \det \left[ I_M + \frac{\sigma}{N} HH^* \right] \right) \frac{\text{bits}}{\frac{\text{s}}{\text{Hz}}} \tag{4}$$

where  $I_M$  is the  $M \times M$  identity matrix,  $\sigma$  is the average SNR per receive antenna,  $H$  is the channel matrix and  $*$  represents the complex conjugate transpose. The Equation (4) is only applied when  $M < N$ . If  $M > N$ , the term  $HH^*$  is replaced by  $H^*H$ , and  $I_M$  is replaced by  $I_N$ . In addition, for a frequency selective channel, the MIMO channel capacity is obtained through an average over the whole bandwidth [17].

$$C_f = \epsilon_f \left\langle \log_2 \left( \det \left[ I_M + \frac{\sigma}{N} HH^* \right] \right) \right\rangle \frac{\text{bits}}{\frac{\text{s}}{\text{Hz}}} \tag{5}$$

where  $\epsilon_f$  refers to the mathematical expectation over the channel bandwidth. Indeed, in our study, the measured spectrum (BW = 200 MHz) is subdivided in several sub bands, each of length  $\Delta_f = 1$  MHz. then, the channel capacities for the SISO and  $2 \times 2$  MIMO system are calculated for each subband, and then averaged over the 200 MHz bandwidth. The relationship between the average channel capacity for both MIMO and SISO scenarios, and the distance between the transmitter and the receiver is given by Fig. 7.

As expected, there is a clear gain in capacity with MIMO configuration over the classical SISO system. In fact, it is observed

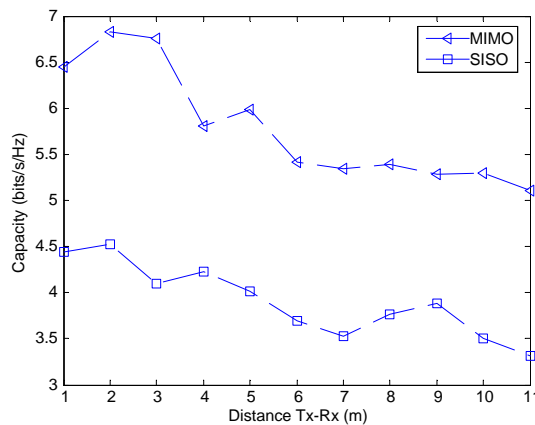


**Figure 7.** Channel capacity for MIMO and SISO configurations.

**Table 3.** MIMO versus SISO channel capacity statistics (bits/s/Hz).

CAPACITY	Min	Max	Mean	Std
MIMO	5.11	6.83	5.78	0.63
SISO	3.32	4.52	3.91	0.39

from the figure above, that  $C_{MIMO}$  is almost all 1.87 bits/s/Hz greater than  $C_{SISO}$ . Hence, this confirms the fact that using more antenna elements provides an increase in terms of channel capacity. Moreover, the highest capacity value within the MIMO configuration is 6.83 bits/s/Hz and is reached at 2 meters from the transmitter where there a little  $k$ -factor ( $k\text{-factor}_{2m} = 3.84$  dB), equivalently less correlation between arriving paths at the receiver. Furthermore, it is shown that minimum capacities are achieved at far distances from the transmitter. Indeed, high path loss as well as rician factor values tend to decrease the channel diversity and then the channel capacity. Table 3 gives a brief glance of the channel capacity statistics.

#### 4. CONCLUSION

This paper deals with MIMO channel characterization obtained from a measurement campaign made around a center frequency of 5.8 GHz in an underground mine gallery. Results show a slightly specific propagation behavior in such underground areas. Indeed, large scale analysis demonstrated that the pathloss exponent inside the mine gallery is close to the free space value. Furthermore, the channel capacity was studied at a fixed transmitted power and variable SNR. Hence, the capacity results will include both effects related to received power and path channel richness. Results show that when using MIMO systems, there is an average gain over SISO channel capacity of about 1.87 bits/s/Hz. In addition, the  $K$ -factor mean value is 5.68 dB which enhances the wireless link in terms of outage probability. Thus, MIMO systems have achieved better performances over SISO channels, and then can present a good candidate for future wireless underground communication systems.

#### REFERENCES

1. Ben Mabrouk, I., L. Talbi, M. Nedil, and K. Hettak, "MIMO-UWB channel characterization within an underground mine gallery", *IEEE Transactions on Antennas and Propagation*, Vol. 60, 4866–4874, Oct. 2012.

2. Shin, H. and J. H. Lee, "Capacity of multiple-antenna fading channels: Spatial fading correlation, double scattering, and keyhole," *IEEE Transactions on Information Theory*, Vol. 49, 2636–2647, Oct. 2003.
3. Foschini, G. J. and M. J. Gans, "On limits of wireless communications in a fading environment," *Wireless Pers. Commun.*, Vol. 6, 311–335, 1998.
4. Tarokh, V., N. Seshadri, and A. R. Calderbank, "Space-time codes for high data rate wireless communication: Performance criterion and code construction," *IEEE Transactions on Information Theory*, Vol. 44, 744–765, Mar. 1998.
5. Yu, K., M. Bengtsson, B. Ottersten, D. McNamara, P. Karlsson, and M. Beach, "Modeling of wide-band MIMO radio channels based on NLoS indoor measurements," *IEEE Transactions on Vehicular Technology*, Vol. 53, 655–665, May 2004.
6. Molisch, A. F., M. Steinbauer, M. Toeltsch, E. Bonek, and R. S. Thoma, "Capacity of MIMO systems based on measured wireless channels," *IEEE Journal on Selected Areas in Communications*, Vol. 20, 561–569, Apr. 2002.
7. Boutin, M., A. Benzakour, C. L. Despins, and S. Affes, "Radio wave characterization and modeling in underground mine tunnels," *IEEE Transactions on Antennas and Propagation*, Vol. 56, 540–549, Feb. 2008.
8. Jakes, W. C., *Microwave Mobile Communications*, Wiley, New York, 1974.
9. Tepedelenlioglu, C., A. Abdi, and G. Giannakis, "The ricean  $K$  factor: Estimation and performance analysis," *IEEE Transactions on Wireless Communications*, Vol. 2, No. 4, 799–810, 2003.
10. Khan, I. and P. S. Hall, "Experimental evaluation of MIMO capacity and correlation for narrowband body-centric wireless channels," *IEEE Transactions on Antennas and Propagation*, Vol. 58, No. 1, 195–202, Jan. 2010.
11. Ben Mabrouk, I., L. Talbi, B. Mnasri, M. Nedil, and N. Kandil, "Experimental characterization of a wireless MIMO channel at 2.4 GHz in underground mine gallery," *Progress In Electromagnetics Research Letters*, Vol. 29, 97–106, 2012.
12. Sarris, I. and A. R. Nix, "Ricean  $K$ -factor measurements in a home and an office environment in the 60 GHz band," *Mobile and Wireless Communications Summit*, 2007.
13. Ben Mabrouk, I., L. Talbi, M. Nedil, and K. Hettak, "MIMO-UWB channel characterization within an underground mine

- gallery,” *IEEE Transactions on Antennas and Propagation*, Vol. 60, No. 10, 4866–4874, Jul. 2012.
14. Karedal, J., S. Wyne, P. Almers, F. Tufvesson, and A. F. Molisch, “A measurement-based statistical model for industrial ultra-wideband channels,” *IEEE Transactions on Wireless Communications*, Vol. 6, 3028–3037, Aug. 2007.
  15. Telatar, I. E., “Capacity of multi-antenna Gaussian channels,” *European Trans. Telecommun. (ETT)*, Vol. 10, No. 6, 585–595, Nov./Dec. 1999.
  16. Maaref, A. and S. Aissa, “On the capacity statistics of MIMO Ricean and rayleigh fading channels,” *IEEE International Conference on Communications*, Vol. 9, 4167–4172, Jun. 2006.
  17. Mabrouk, I. B., L. Talbi, M. Nedil, Y. Coulibaly, and T. A. Denidni, “Effect of antenna directivity on performance of multipleinput multiple output systems in an underground gold mine,” *IET Microw. Antennas Propag.*, Vol. 6, No. 5, 555–561, Apr. 12, 2012.